Supporting Information

Coordinating Zincophilic Sites and Solvation Shell for Dendrite-free Zn Anode under Synergistic Effects of Polyacrylonitrile and Dimethyl Sulfoxide

Zhenjie Liu, Jiale Ma, Xiangjian Liu, Haiyang Wu, Dianlun Wu, Bin Chen, Peng Huang, Yang Huang, Lei Wang, Zhenyu Li,* Shulei Chou**

Dr. Z. Liu and Dr. J. Ma contributed equally to this work.

Materials.

Zinc trifluoromethane sulfonate ($Zn(OTF)_2$, 98%), Polyacrylonitrile (PAN, average Mw 85000), Dimethyl sulfoxide (DMSO, spectrum grade, ≥99.9%) and Zn foil (thickness:0.8 cm) were purchased from Aladdin Biochemical Technology Co., Ltd. Chemical Company. Ti foil (thickness:0.5 cm) and Ti mesh (200 mesh) were purchased from Xinshuo Scientific Research Metal Materials Co., Ltd. The NaV_3O_8 $1.5H_2O$ (NVO) cathode were synthesized *via* a conventional route according to a previous study.[1,2]

Preparation of the hybrid electrolyte and symmetrical batteries assembly.

The hybrid electrolytes were prepared by dissolving $Zn(OTF)_2$ and PAN with a predetermined molar ratio in DMSO-H_2O solution (1:1 volume ration). The concentration of the $Zn(OTF)_2$ is 1.0 M, and the concentration of the PAN in the mixture electrolytes was controlled by the mass ratio (0.2%). In addition, PAN molecular is insoluble in pure water, which is also responsible for the introduction of DMSO in the electrolytes.

All the batteries were assembled using CR2032 coin-type cell. The cathodes were prepared by mixing the NVO, ketjen black and polyvinylidene fluoride (m/m: 7/2/1) to produce a slurry and paste it on a titanium mesh with a doctor blade. The mass loading of the prepared cathode material is approximately 0.5 mg/cm^{-2}, and the cathode material were dried under vacuum at 80℃ for 12 h before use. Glass microfiber filters membrane (Whatman) was used as a separator. The obtained electrodes from Zn | Zn symmetrical batteries were thoroughly rinsed with alcohols and deionized aqueous solution to remove residual electrolyte.

Electrochemical and measurements.

The cycle stability of the Zn anode was investigated by using a Zn | Zn symmetrical cell and the cycling efficiency of the Zn anode was quantified with a Zn | Ti half cell. Voltammetric study (CV, LSV, EIS and Tafel) of the electrolytes was performed with a CHI electrochemical workstation (CHI760E) using Zn | Zn cell or Zn | Ti cell, respectively. The EIS for ZIBs was performed at the frequency range of 0.01−100000 Hz. Galvanostatic tests of the assembled cells were performed with a Land CT2001A battery test system. Ionic conductivity was measured by AC impedance spectroscopy in the frequency range 100 mHz to 100 kHz at an AC amplitude of 10 mV. The two electrolytes were added into the electrochemical cell to form a structure of "steel | electrolyte | steel." Ionic conductivity σ was calculated according to the following equation:

$$\sigma = \frac{L}{A\,R_b}$$

where L is the thickness of the Glass microfiber filters membrane, that is to say, the distance between the two stainless electrodes equal to 0.042 cm; A is the area of the electrode equal to 2.011 cm^2. Resistance (R_b) was taken at the intercept of the Nyquist plot with the real axis of the impedance spectra.

Instruments and characterization.

The XPS data were acquired with an ESCALAB 250Xi (Thermo Fisher) system using the Al-Kα (8.34 Å) source under high-vacuum. XRD study of the cathodes was conducted with a Bruker D8 Advance powder X-ray diffractometer with the Cu Kα radiation (λ = 1.54 Å). Raman Spectroscopy was performed by using a customized LabRAM HR Evolution Raman system (HORIBA Scientific) with an excitation wavelength of 532 nm. SEM (Hitachi S-4700) and TEM (FEI Tecnai G2 spirit) were employed to investigate the morphologies of the samples. The ^{67}Zn nuclear magnetic resonance (NMR) experiments were recorded by using a Bruker 600 MHz AVANCEIII spectrometer.

Computational Details.

Spin polarized density functional theory calculations were performed with Vienna Ab-initio Simulation Package (VASP)[3,4] using projector-augmented wave (PAW) pseudopotentials[5] and Perdew-Burke-Ernzerhof (PBE) functional[6]. Electrons in the states of

(3d, 4s) of Zn, (3s, 3p) of S, (2s, 2p) of C, N and O, (1s) of H were considered as valence electrons. The cutoff energy for the plane-wave basis was 520 eV. A set of 3 × 3 × 1 k-point mesh was used to sample the Brillouin zones of adsorption systems. On the other hand, one gamma k-point was used in the calculation of binding energy between the Zn ion and molecule. The convergence for electronic energy and structural optimization was set to be 1E-5 eV and 0.02 eV/Å. The adsorption behaviors of molecules and polymer PAN were simulated on a 4 × 4 Zn surface slab (64 atoms), with one bottom layer fixed and three surface layer relaxed. To break the periodic boundary condition in normal direction of electrode surface, vacuum region with its thickness larger than 20 Å was introduced. In the meantime, with the help of periodic boundary condition in lateral direction, a complete polymer chain was simulated, instead of using a monomer or dimer structure.

The adsorption energy E_{ad} was calculated by:

$$E_{ad} = E_{surf\text{-}mol} - E_{surf} - E_{mol}$$

where $E_{surf\text{-}mol}$ is the energy of Zn surface with adsorbed molecule, E_{surf} is the energy of clean surface slab and E_{mol} is the energy of an isolated molecule. Similarly, the binding energy E_b was calculated by:

$$E_b = E_{ion\text{-}mol} - E_{ion} - E_{mol}$$

where $E_{ion\text{-}mol}$ is the energy of an Zn ion and a molecule interacting with each other, E_{ion} and E_{mol} are the energies of an isolated Zn atom and molecule, respectively.

References

[1] F. Wan, L. Zhang, X. Dai, X. Wang, Z. Niu and J. Chen, *Nat. Commun*. 2018, **9**, 1656.

[2] H.-Y. Wu, X. Gu, P. Huang, C. Sun, H. Hu, Y. Zhong, C. Lai, *J. Mater. Chem. A*. 2021, **9**, 7025-7033.

[3] G. Kresse, J. Furthmüller, *Comput. Mater. Sci.* 1996, **6**, 15-50.

[4] G. Kresse, J. Furthmüller, *Phys. Rev. B* 1996, **54**, 11169-11186.

[5] G. Kresse, D. Joubert, *Phys. Rev. B* 1999, **59**, 1758-1775.

[6] J. P. Perdew, K. Burke, M. Ernzerhof, *Phys. Rev. Lett.* 1996, **77**, 3865-3868.

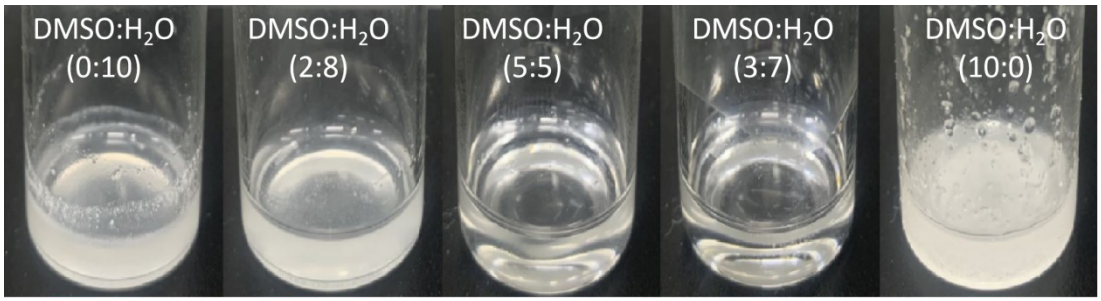

Figure S1. Digital photographs of the PAN-DMSO-H_2O electrolytes with different amounts of DMSO. From left to right, the volume content of DMSO in the electrolyte is 0, 20, 50, 70, and 100%, respectively. It is noted that the total volume is calculated by adding the used volumes of DMSO and H_2O together, while PAN and $Zn(OTF)_2$ are neglected.

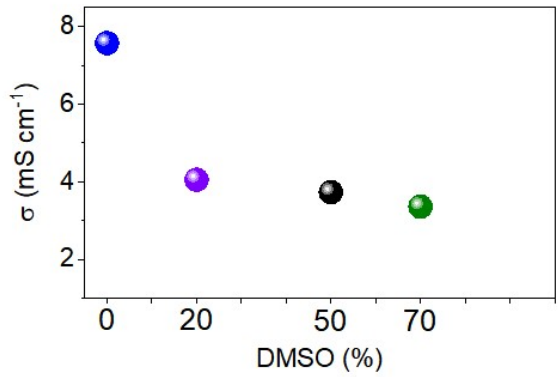

Figure S2. Ionic conductivities of the PAN-DMSO-H_2O electrolytes with different amounts of DMSO. It is noted that there is no PAN addictive in the pristine aqueous electrolyte (*i.e.* 2M $Zn(OTF)_2$ H_2O, blue dot), since PAN is insoluble under this condition.

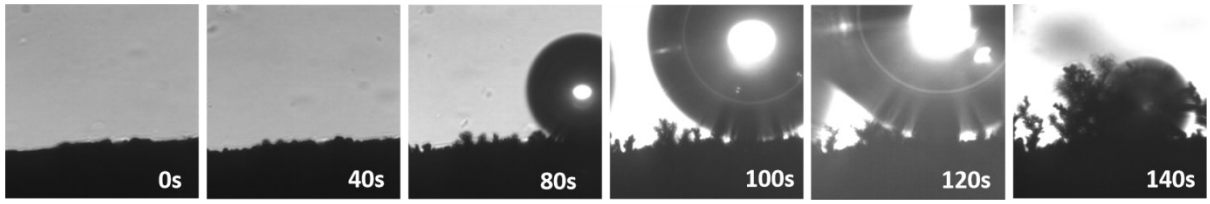

Figure S3. *In-situ* side view of the Zn anode in a pristine aqueous electrolyte during the plating process.

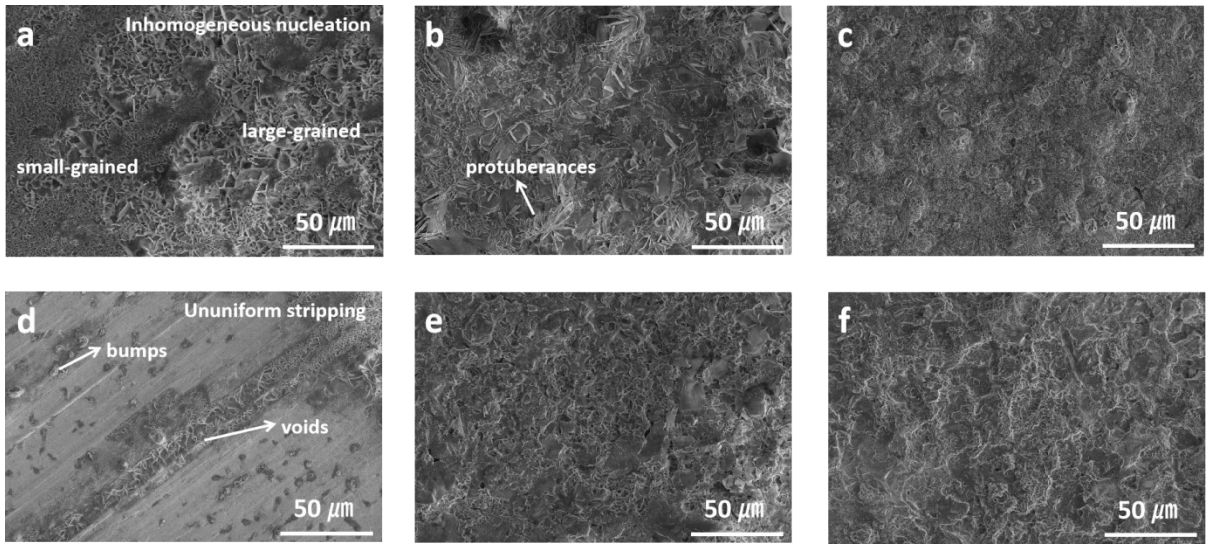

Figure S4. SEM images of Zn anodes after (a-c) plating and (d-f) corresponding stripping processes using different electrolytes: (a, d) pristine aqueous, (b, e) DMSO-H_2O and (c, f) PAN-DMSO-H_2O electrolytes.

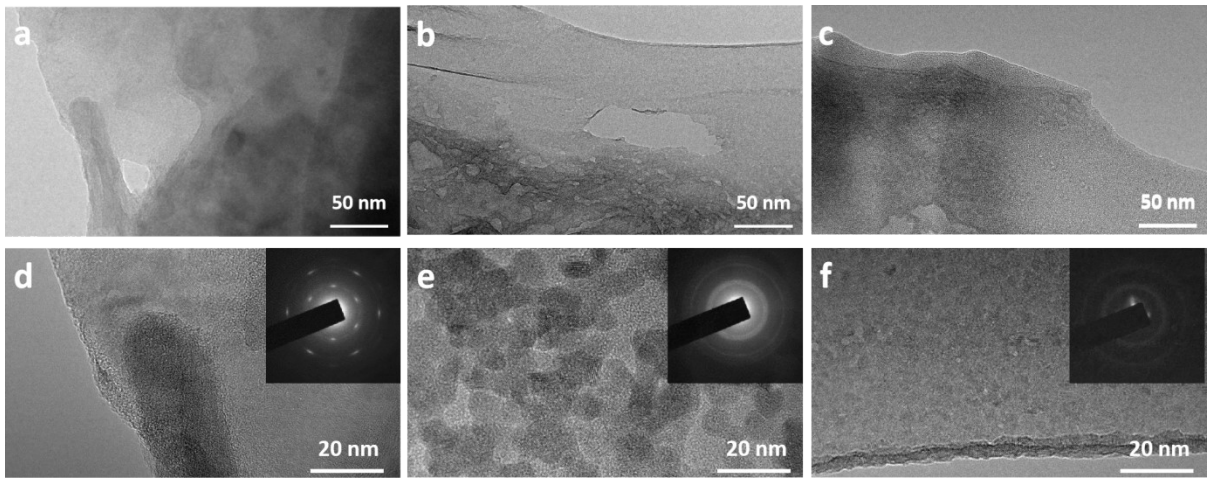

Figure S5. TEM images of the Zn particles obtained after plating process using different electrolytes: (a, d) pristine aqueous, (b, e) DMSO-H_2O and (c, f) PAN-DMSO-H_2O electrolytes. Insets are the selected area electron diffractions of the corresponding TEM images.

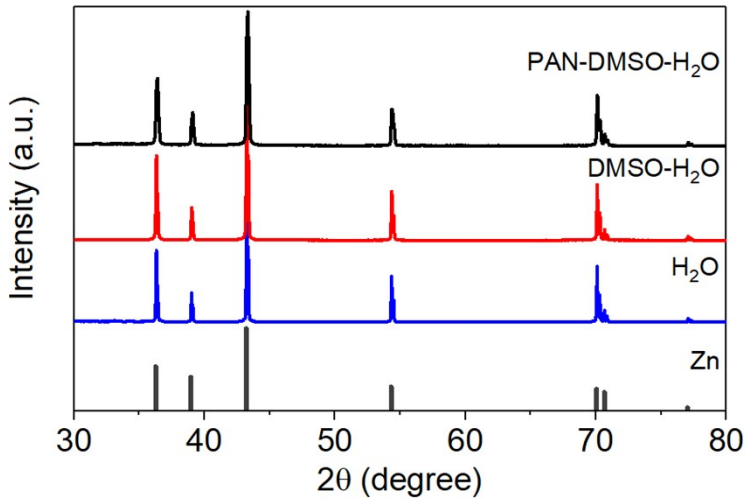

Figure S6. XRD patterns of the plated Zn anodes in different electrolytes.

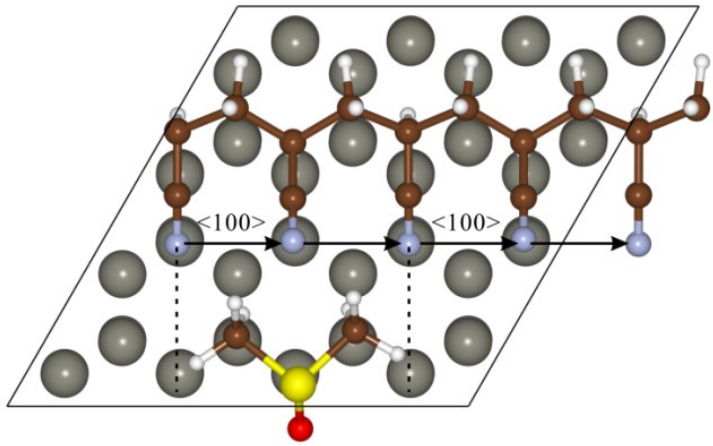

Figure S7. The comparison of chemisorption of PAN and DMSO molecules on Zn (0001) facet.

Figure S8. The contact angles between Zn metal and different electrolytes.

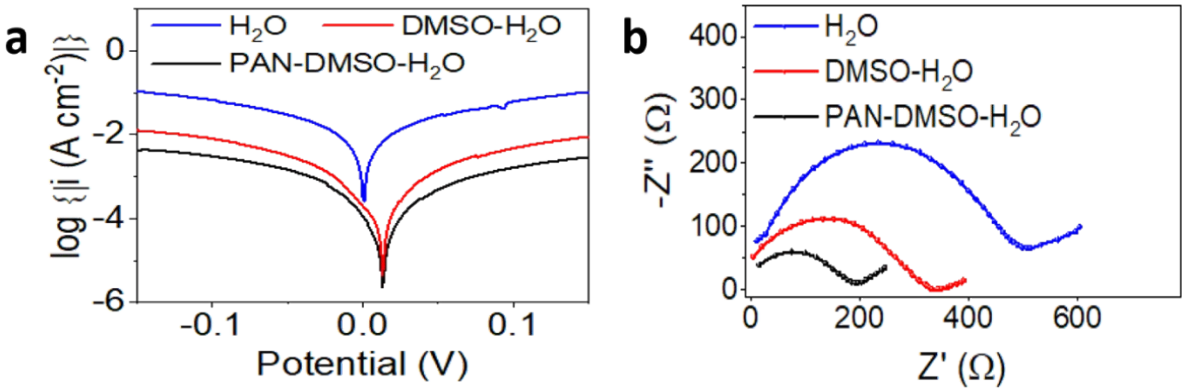

Figure S9. (a) Tafel plots obtained from the Zn | Zn symmetric batteries with a scan rate of 1.0 mV s^{-1} after resting for one day, and their (b) electrochemical impedance spectroscopy (EIS) in different electrolytes.

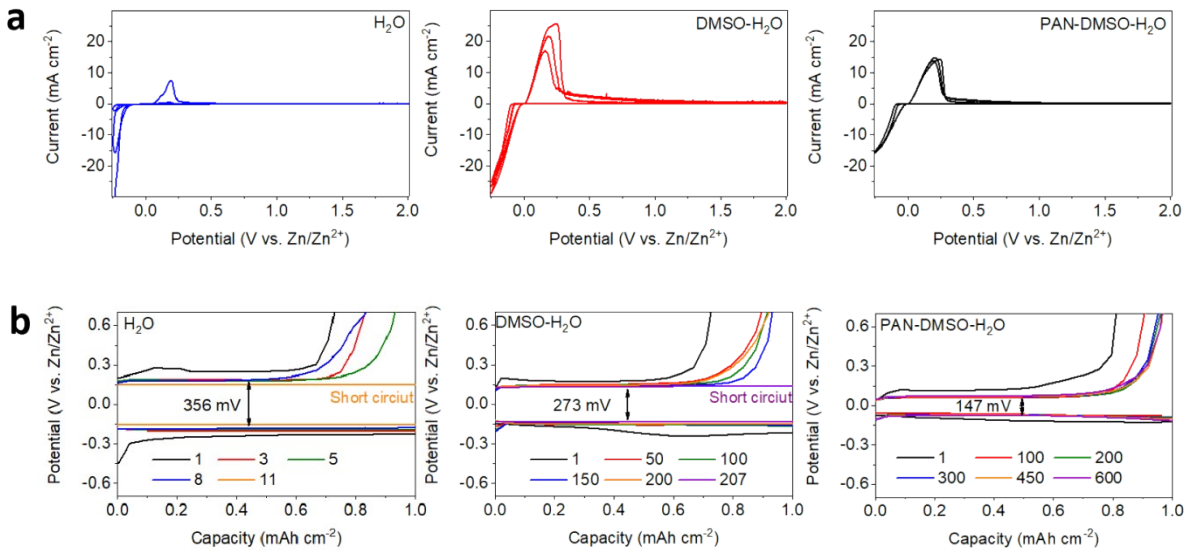

Figure S10. (a) Cyclic voltammetry (CV) curves of the Zn plating/stripping in different electrolytes at a scan rate of 1.0 mV s^{-1}. (b) Galvanostatic Zn plating/stripping curves in different electrolytes at a current density of 5.0 mA cm^{-2} and an areal capacity of 1.0 mAh cm^{-2}.

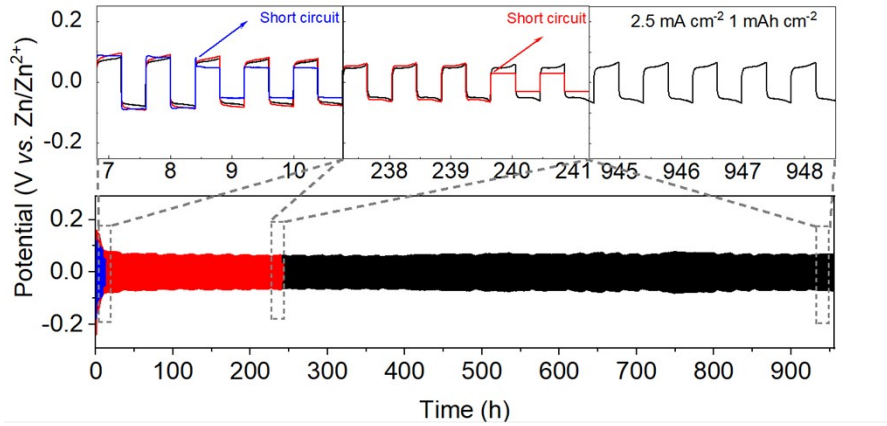

Figure S11. Cycling performance of Zn | Zn symmetric batteries containing different electrolytes at a current density of 2.5 mA cm^{-2} and an areal capacity of 1.0 mAh cm^{-2}.

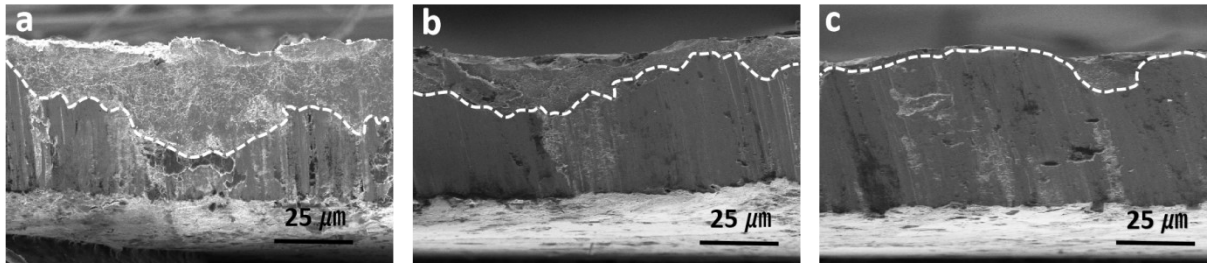

Figure S12. Cross-section SEM images of the Zn anodes after 100 cycles of plating/stripping with (a) pristine aqueous, (b) DMSO-H_2O and (c) PAN-DMSO-H_2O electrolytes, respectively.

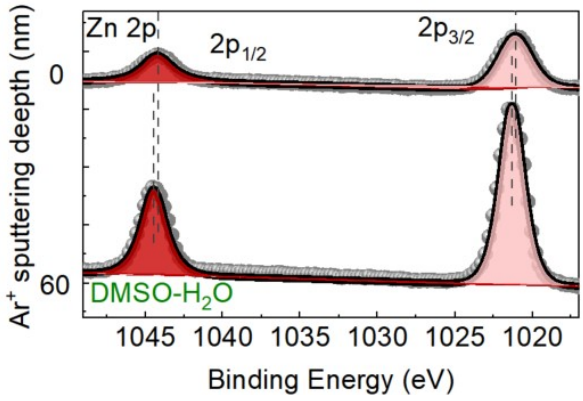

Figure S13. Zn 2p XPS spectra of the cycled Zn anodes in DMSO-H_2O electrolyte. The Zn anode harvested from Zn | Zn symmetric batteries were cycled at 5.0 mA cm^{-2} for 100 cycles.

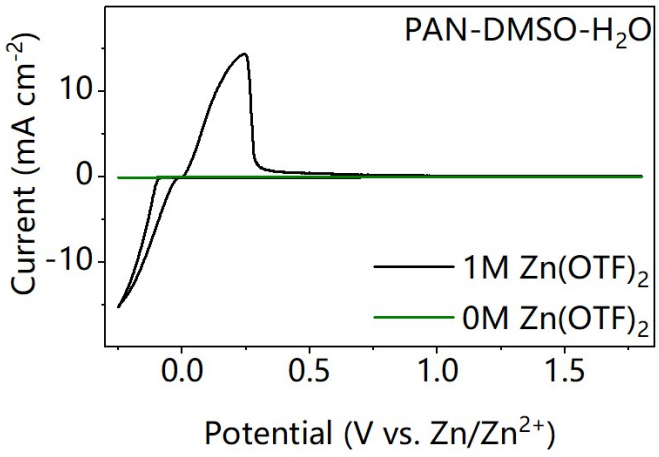

Figure S14. CV curves of the Zn | Ti batteries in the electrolytes with/without Zn salt at a scan rate of 1.0 mV s^{-1}. It is noted that no faraday current is observed in the test voltage window without Zn salt (*i.e.* green line), indicating that no redox reaction occurs in the electrolyte. In other words, PAN should be stable in the electrolyte during Zn plating/stripping.

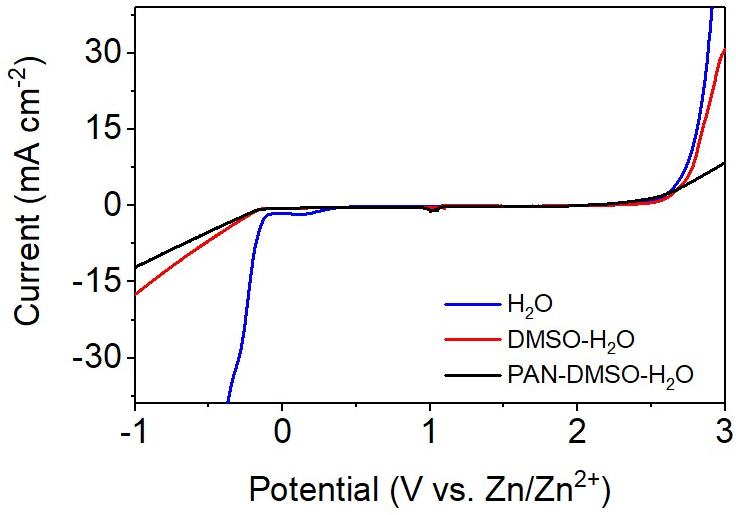

Figure S15. The electrochemical stability window of the pristine aqueous (blue line), DMSO-H_2O (red line) and PAN-DMSO-H_2O (black line) electrolytes obtained by linear sweep voltammetry at 5 mV s^{-1}.

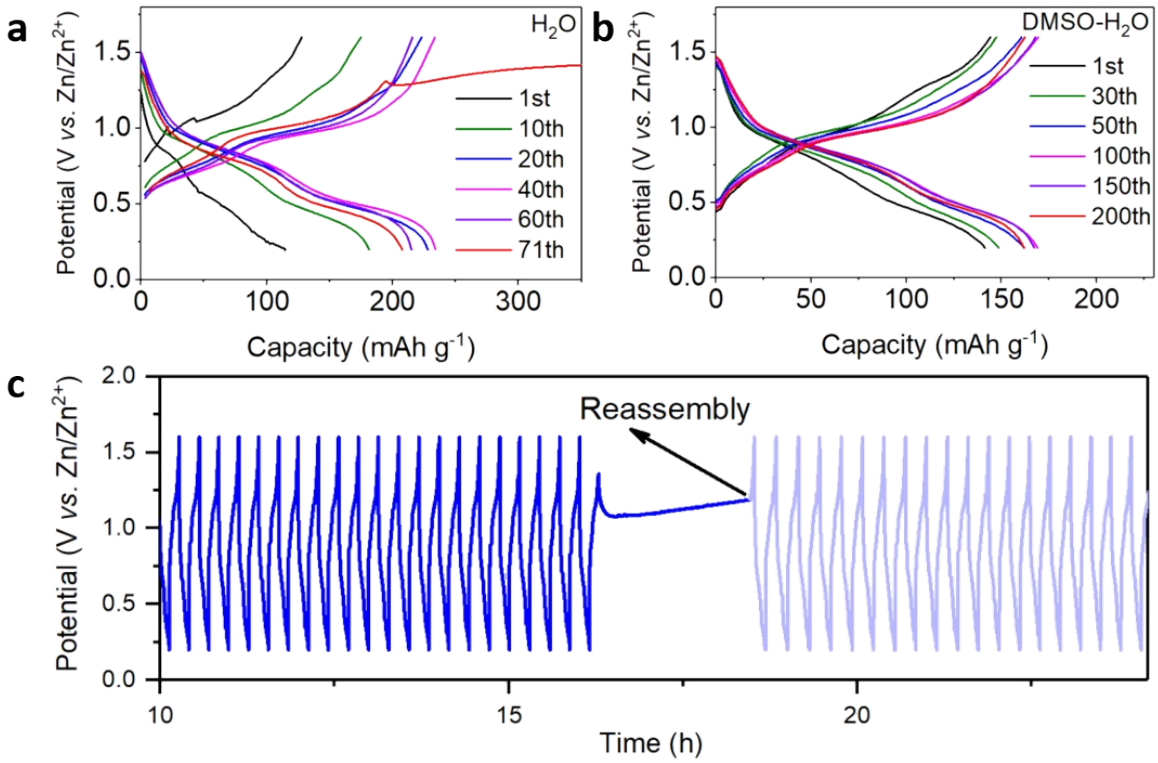

Figure S16. Galvanostatic charge-discharge curves at a current density of 1 A g^{-1} in the (a) pristine aqueous and (b) DMSO-H_2O electrolyte. And restoration curves after replacing a new Zn anode in (c) pristine aqueous electrolyte.